DEM Generation with SAR Interferometry Based on Weighted Wavelet Phase Unwrapping

Maryam Rahnemoonfar, Beth Plale

School of Informatics and Computing
Indiana University Bloomington, USA
maryrahn@indiana.edu

Abstract-Synthetic aperture radar Interferometry (InSAR) is a significant 3D imaging technique to generate a Digital Elevation Model (DEM). The phase difference between the complex SAR images displays an interference fringe pattern from which the elevation of any point in the imaged terrain can be determined. Phase unwrapping is the most critical step in the signal processing of InSAR and especially in DEM generation. In this paper, a least squares weighted wavelet technique is used which overcomes the problem of slow convergence and the less-accurate Gauss-Seidel method. Here, by decomposing a grid to low-frequency and high-frequency components, the problem for a low-frequency component is solved. The technique is applied to ENVISAT ASAR images of Bam area. The experimental results compared with the Statistical-Cost Network Flow approach and the DEM generated from a 1/25000 scale map of the area shows the effectiveness of the proposed method.

Keywords- DEM, InSAR, Phase unwrapping, wavelet

I. INTRODUCTION

The digital elevation model (DEM), one of the most essential data in geo-spatial analysis, traditionally has been created by using optical stereo images taken from aircrafts and satellites. One of the obstacles in the creation of DEMs using optical images is their dependence on weather and daylight. Thanks to its active system and its long wavelength, radar is able to acquire the data at any time, day or night, regardless of weather conditions.

Interferometric Synthetic Aperture Radar (InSAR) is a technique that uses two or more complex SAR images taken with a time delay and/or cross-track parallax, to infer height or motion information about the Earth's surface. Some significant applications of InSAR techniques are DEM generation [1], earthquake monitoring [2], land use classification [15] and glacier velocity measurements [10].

The InSAR DEM generation is based on the processing of at least two complex SAR images which cover the same area and are acquired with two antennas separated by a baseline. In order to generate a DEM several processing stages are necessary: namely image registration, interferogram calculation and filtering, phase unwrapping and phase-to-height transformation. The most complex and critical stage of the entire procedure is phase unwrapping. Due to the nature of SAR imaging, the phase is given in modulo 2π and there is an ambiguity in calculating the correct integer number of 2π phase cycles. This ambiguity solution is referred to as phase unwrapping and is an important stage in the derivation of elevations using the InSAR technique.

The problem of phase unwrapping has been the focus of InSAR research for several years. Numerous methods were proposed and implemented for this most complex issue of the interferometric processing chain. The two major approaches are "path-following" and "least-squares" algorithms. Path-following algorithms [5, 7, 8] use localized pixel-by-pixel operations to unwrap the phase, while least-squares algorithms [6, 11, 13] minimize a global measure of the differences between the gradients of the wrapped input phase and those of the unwrapped solution. In recent years significant advances have been made using the network approach [3], multi-resolution approach [4] and wavelet [9, 14]. Wavelet technique [9, 14] was applied only on simulated data.

In this paper, weighted wavelet technique is used for the phase unwrapping step by InSAR technique. Wavelet phase unwrapping was briefly introduced in our previous work [14] where the proposed method was applied only on simulated data. In this paper the proposed phase unwrapping approach is applied on real data, and is then evaluated by comparing the result with a DEM generated from a 1/25000 scale map of the area, as well as with the network approach [4]. In addition, in this paper a post-processing step is applied to the wavelet unwrapped phase in order to ensure the congruency of the unwrapped phase to the wrapped phase. Another correction model is also introduced to remove the error - caused by atmosphere, phase and baseline - and to improve the accuracy of the generated DEM.

The first part of this paper describes a complete InSAR procedure, while giving particular emphasis to the phase unwrapping step. A rigorous approach for phase unwrapping using weighted wavelet phase unwrapping is presented. In the second part of the paper, the results obtained by processing Envisat images are analyzed. Two DEMs are validated using a suitable reference DEM, derived by aerial photogrammetry as a byproduct of 1:25000 topographic maps.

II. InSAR PROCESSING STEPS

The main processing steps of InSAR are shown in Fig. 1.

Fig. 1. Main processing steps of InSAR

The first step of a typical InSAR processing routine is the co-registration of the slave image over the master one. This step accounts for different sensor attitudes, orbit skewing and along-track and across-track shifts. Imprecise alignment of the two images causes a coherency loss between the two interferometric signals which has a great influence on the quality of DEM.

In the second step the Interferogram is computed by multiplying the complex value of each pixel of the master image by the conjugate complex of the corresponding pixel in the slave image. This Interferogram should undergo "flat earth correction" which is the removal of strong contribution due to the slant range geometry using the orbit data.

Once the Interferogram has been calculated, the next important and critical step in the interferometric processing is the phase unwrapping. This stage will be discussed in further detail in the next section.

After the phase unwrapping step, the unwrapped phase is converted to height with the following formula:

$$dh = \frac{-\lambda}{4\pi} \cdot \frac{r \sin\theta}{B_h \cos\theta - B_v \sin\theta} d\varphi \qquad (1)$$

where φ is the unwrapped phase, B_h and B_v are the horizontal and vertical components of the baseline, θ is the look angle, r is the slant range and h is the height above reference ellipsoid. After a phase to height conversion and a geocoding process, the digital elevation model can be extracted.

A. Wavelet Phase Unwrapping

The phase obtained by SAR interferometry is wrapped because the arctangent is defined over a range from $-\pi$ to π.

Phase unwrapping must be performed to obtain the true phase. In this paper the phase is unwrapped using a phase unwrapping algorithm based on the least-squares wavelet transform. It is assumed that the phase of interferogram, $\psi_{i,j}$ which is between $-\pi$ and π is known. We want to determine the unwrapped phase value $\varphi_{i,j}$

$$\psi_{i,j} = \varphi_{i,j} + 2\pi k \qquad (2)$$

The weighted least square approach attains the unwrapped phase by minimizing the difference between the discrete partial derivatives of the wrapped phase and the discrete partial derivatives of the unwrapped solution. The solution $\varphi_{i,j}$ that minimizes $\mathcal{L}$ is the weighted least square solution, where $\mathcal{L}$ is

$$\mathcal{L} = \sum_i \sum_j w_{i,j}^x (\varphi_{i,j} - \varphi_{i-1,j} - \Delta x_{i,j})^2$$
$$+ \sum_i \sum_j w_{i,j}^y (\varphi_{i,j} - \varphi_{i,j-1} - \Delta y_{i,j})^2; \qquad (3)$$

where w^x and w^y are weight functions and Δx and Δy are the partial derivatives of the wrapped phase:

$$\Delta x_{i,j} = W\{\psi_{i+1,j} - \psi_{i,j}\},$$
$$\Delta y_{i,j} = W\{\psi_{i,j+1} - \psi_{i,j}\}, \qquad (4)$$

where W is the wrapping operator. The least squares solution of (3) yields the following equation

$$w_{i,j}^x (\varphi_{i+1,j} - \varphi_{i,j}) - w_{i-1,j}^x (\varphi_{i,j} - \varphi_{i-1,j})$$
$$+ w_{i,j}^y (\varphi_{i,j+1} - \varphi_{i,j}) - w_{i,j-1}^x (\varphi_{i,j} - \varphi_{i,j-1}) = \rho_{i,j}, \qquad (5)$$

where

$$\rho_{i,j} = w_{i,j}^x \Delta x_{i,j} - w_{i-1,j}^x \Delta x_{i-1,j} + w_{i,j}^y \Delta y_{i,j} - w_{i,j-1}^y \Delta y_{i,j-1}). (6)$$

Equation (5) is a weighted and discrete version of the Poisson's partial differential equation (PDE) which in matrix format yields the following equation:

$$A\varphi = \rho \qquad (7)$$

where A is a sparse matrix and φ is the solution of phase unwrapping. Solving the Poisson's equation with the classical method of Gauss-Seidel relaxation has extremely slow convergence. Wavelet techniques overcome this limitation by transforming low-frequency components of error into high-frequency components which consequently can be removed quickly by using the Gauss-Seidel relaxation method.

In Discrete Wavelet Transform (DWT) two operators, decomposition (analysis) and reconstruction (synthesis), are used. In the decomposition stage an image is separated into one low-frequency component (approximation) and three high-frequency components (details). In the reconstruction stage, the image is reconstructed by synthesizing the approximated and detail components.

For solving (7) by wavelet algorithm, after relaxing v_1 times on the equation (7) with the initial guess φ_0, the residual error of this equation is transformed by the decomposition step of DWT into coarser grid. Then, further relaxation is performed on the residual equation $Ae = r$ in the low-frequency component of the coarser grid with the initial guess $e = 0$, where $r = \rho - A\hat{\varphi}$ is the known residual error. The resulting solution of the lower component of the coarser grid is regarded as an intermediate solution whose residual error is transformed to the next coarser grid with DWT. This process continues until we reach the coarsest grid. At this

88

point the solution is then transferred to the finer grid by the reconstruction analysis of DWT; ultimately, it will be added to the approximation $\hat{\phi}$. This process yields a better solution on the finer grid. The weight array is embedded in matrix A so that the decomposition and reconstruction of weights array are conducted in parallel. Weights for real data will be defined in the next section. Because the least-squares solution minimizes the squares of the differences between the gradients of the solution and the phase, the solutions are not congruent to the wrapped phase [12]. Therefore, after solving (7) with a wavelet algorithm, it is necessary to perform a post-processing step by subtracting the solution from the wrapped input phase, rewrapping the result, and then adding it back into the solution.

III. EXPERIMENTAL RESULTS

In this research, two single look complex SAR images of ENVISAT ASAR data are used which were made available by the European Space Agency used for DEM generation (Fig. 2). These images cover an area about $100km$ by $100km$ of Bam, Fahraj, Nosratabad and Sabzevaran cities in the Kerman province of Iran.
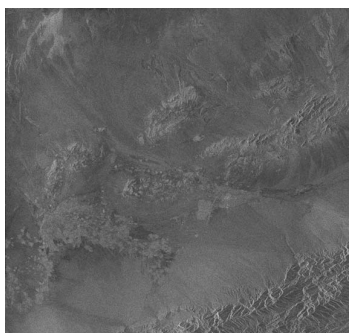

Fig. 2. SAR image of study area

The first two processing stages, namely co-registration and interferogram generation, were performed using the freely available Doris software package [8]. The filtered interferograms were unwrapped using the weighted wavelet algorithm explained in the previous section. For Weight function we used the coherence map of the area. The same weight function was used for both x and y directions. After the phase unwrapping step by weighted wavelet algorithm, the post-processing step is also performed to achieve congruence between the unwrapped phase and the wrapped phase. In order to construct the DEM, the unwrapped phases were converted to height and then geo-coded. Figure 3 shows the final DEM result.
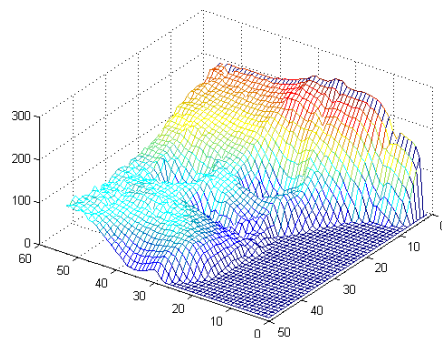

Fig. 3. 3D model of the area produced by InSAR

To evaluate the results, the weighted phase unwrapping algorithm was compared to a network phase unwrapping approach [3]. In addition, the DEM generated as the result of InSAR processing was compared with a DEM generated from a 1/25000 scale map. The evaluation was performed in two regions of the Kerman province, namely Fahraj and Nosratabad, due to reference DEM availability in these two regions.

Figure 4 shows the interferograms and the deference between heights produced by the unwrapped phase, using the wavelet and the network approach in these two regions. Figure 4.b shows the coherence map of the Nosratabad region which was used as a weight function for that area. A similar weight function is also used for the Fahraj region. It can be seen from figure 4.c and 4.e that the difference between heights in the two phase unwrapping methods is less than 5cm in Fahraj and less than 13 cm in Nosrataabd region.
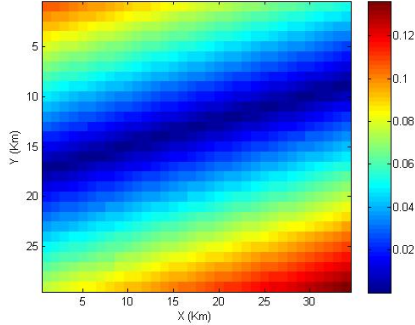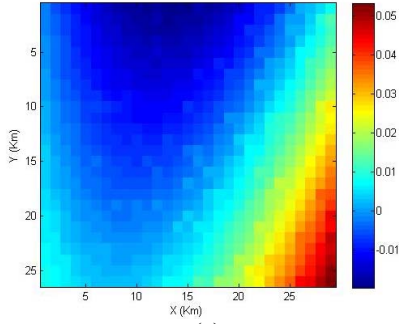

(a)

(b)

89
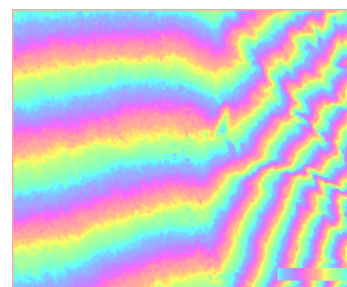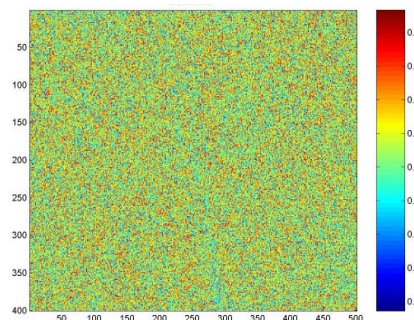
(c)

(d)

(e)

Fig. 4. (a, d) Interferogram for Nosraaabad and Fahraj regions, (b) weight function for Nosratabad region (c ,e) the difference (in meter) between height obtained by wavelet and network phase unwrapping methods [3] for Nosratabad and Fahraj regions

To compare the result of the DEM generated by SAR interferometry with the reference topographic map, at least one ground control point (GCP) is required to shift the InSAR DEM due to the constant of integration in phase unwrapping and phase to height transformation steps. In fact, other parameters (1) affect the accuracy of the final DEM. Phase and baseline are two important parameters that influence the DEM accuracy. The behaviors of these two parameters are significantly different in nature. The phase errors increase the statistical variation of each point in the DEM, while the baseline errors are systematic. In order to reduce the errors we proposed the following polynomial which is experimentally recognized as the best model to remove errors due to the phase, baseline and atmosphere.

$$\Delta z = a_0 + a_1 x + a_2 y + a_3 x^2 \qquad (8)$$

In the above equation, Δz is the difference between interferometric height and topographic height; (x, y) is the coordinate of the control point. To determine the unknown parameters (a_0, a_1, a_2, a_3), 9 ground control points were selected with known coordinates in both models. The constant coefficient a_0 represents the constant of integration in the phase unwrapping and phase to height transformation steps, as well as the constant shift due to atmosphere error. Linear coefficients (a_1 and a_2) represent orbital error as well as error due to ionosphere and troposphere. Quadratic coefficient a_3 represents the atmospheric error. After determining unknown parameters a_0 to a_4 with 9 control points, Δz was added to interferometric heights. At the next step the accuracy of interferometric heights compared with reference DEM on around 1000 check points in each region. Figure 5 shows the position of control points (GCPs) and check points for Fahraj region.
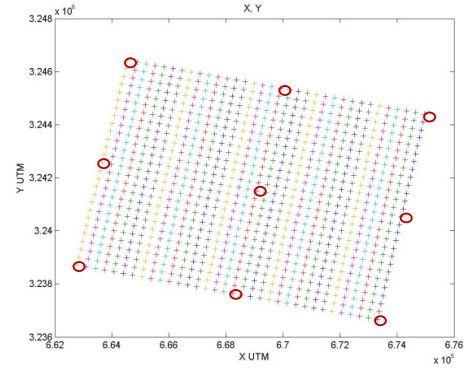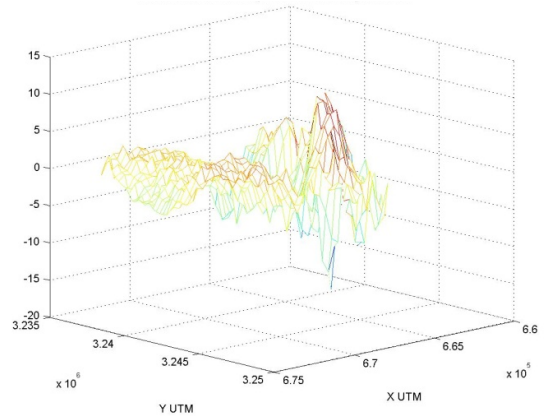

Fig. 5. Position of check points and 9 control points in Fahraj region

Fig 6 shows the height difference between the DEM generated by the interferometric model and the reference DEM for two regions.
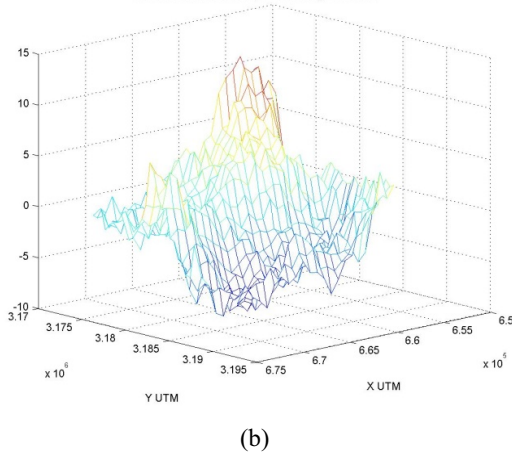

(a)

90

(b)

Fig. 6. Difference between height value of interferometric model acquired with wavelet phase unwrapping and reference DEM on all check points for (a) Nosrataabd and (b) Fahraj

Table 1 shows the average amount of height difference between the DEM produced by SAR Interferometry and the reference DEM. The InSAR DEMs of both regions, obtained using two different approaches, are first compared with the reference DEM without any correction (only by shifting the whole model with 1 GCP to solve the constant of integration); next, they are compared with the correction model in equation (8) and with 9 GCP.

TABLE 1. THE DIFFERENCE BETWEEN HEIGHT WITH
INTERFEROMETRIC MODEL AND REFERENCE DEM (in meter)

	Wavelet	Network approach [3]
Fahraj	22.748	22.735
Norsratabad	4.051	4.024
Fahraj-after correction by equation (8)	**3.055**	**3.058**
Norsratabad-after correction by equation (8)	**2.601**	**2.556**

Comparing the InSAR DEMs of the two regions, it is observable that the calculated DEM of the Nosratabad region is more accurate than the Fahraj region even before correction. This is due to the fact that the average coherency in Nosratabad is 0.57, while it is only 0.41 for the more mountainous Fahraj region. The accuracy obtained after correction is about 3 meters in accordance with the reported accuracy of other InSAR DEMs [16].

IV. CONCLUSION

SAR interferometry was used for DEM generation with a new and faster procedure of wavelet phase unwrapping. Excellent agreement between the wavelet approach and other phase unwrapping techniques was obtained. In addition, good agreement between our technique and the DEM generated by a map of 1/25000 scale was achieved.

REFERENCES

[1] Abdelfattah, R., and Nicolas, J.M., "Topographic SAR interferometry formulation for high-precision DEM generation", *IEEE Transactions on Geoscience and Remote Sensing*, 40, (11), 2002, pp. 2415-2426

[2] Burgmann, R., Rosen, P.A., and Fielding, E.J., "Synthetic aperture radar interferometry to measure Earth's surface topography and its deformation", *Annual Review of Earth and Planetary Sciences*, 28, (1), 2000, pp. 169-209

[3] Chen, C.W., and Zebker, H.A., "Two-dimensional phase unwrapping with use of statistical models for cost functions in nonlinear optimization", *Journal of the Optical Society of America*, 18, (2), 2001, pp. 338-351

[4] Davidson, G.W., and Bamler, R., "Multiresolution phase unwrapping for SAR interferometry", *IEEE Transactions on Geoscience and Remote Sensing*, 37, (1), 1999, pp. 163-174

[5] Flynn, T.J., "Two-dimensional phase unwrapping with minimum weighted discontinuity", *J. Opt. Soc. Amer. A, Opt. Image Sci.*, 14, (10), 1997, pp. 2692-2701

[6] Ghiglia, D.C., and Romero, L.A., "Robust two-dimensional weighted and unweighted phase unwrapping that uses fast transforms and iterative methods", *J. Opt. Soc. Amer. A, Opt. Image Sci*, 11, (1), 1994, pp. 107-117

[7] Goldstein, R., Zebker, H., and Werner, C., "Satellite radar interferometry-Two-dimensional phase unwrapping", *Radio Science*, 23, (4), 1988, pp. 713-720

[8] Gurov, I., and Volkov, M., "Fringe evaluation and phase unwrapping of complicated fringe patterns by the data-dependent fringe processing method", *IEEE Transactions on Instrumentation and Measurement*, 55, (5), 2006, pp. 1634-1640

[9] Kim, S., and Kim, Y.-S., "Least squares phase unwrapping in wavelet domain", *IEE Proceedings Vision, Image and Signal Processing*, 2005, pp. 261-267

[10] Kumar, V., Venkataramana, G., and HÃ¸gda, K., "Glacier surface velocity estimation using SAR interferometry technique applying ascending and descending passes in Himalayas", *International Journal of Applied Earth Observation and Geoinformation*, 13, (4), 2011, pp. 545-551

[11] Pritt, M.D., "Phase unwrapping by means of multigrid techniques for interferometric SAR", *IEEE Transactions on Geoscience and Remote Sensing*, 34, (3), 1996, pp. 728-738

[12] Pritt, M.D., "Congruence in least-squares phase unwrapping", *IGARSS'97*, 1997, pp. 875-877

[13] Pritt, M.D., and Shipman, J.S., "Least-squares two-dimensional phase unwrapping using FFT's", *IEEE Transactions onGeoscience and Remote Sensing*, 32, (3), 1994, pp. 706-708

[14] Rahnemoonfar, M., Rahmati, M., Tavakoli, A., and Saradjian, M., "Two dimensional phase unwrapping of interferometric SAR data by means of wavelet technique", *Proceedings of IEEE International Geoscience and Remote Sensing Symposium (IGARSS'05)*, 2005, pp. 5467-5470

[15] Santoro, M., Wegmuller, U., and Askne, J.I., "Signatures of ERS-Envisat Interferometric SAR Coherence and Phase of Short Vegetation: An Analysis in the Case of Maize Fields", *IEEE Transactions on Geoscience and Remote Sensing*, 48, (4), 2010, pp. 1702-1713

[16] Toutin, T., and Gray, L., "State-of-the-art of elevation extraction from satellite SAR data", *ISPRS Journal of Photogrammetry and Remote Sensing*, 55, (1), 2000, pp. 13-33